Basin Research (2007) **19**, 361–378, doi: 10.1111/j.1365-2117.2007.00330.x

Detrital zircon geochronology of Carboniferous–Cretaceous strata in the Lhasa terrane, Southern Tibet

Andrew L. Leier, Paul Kapp, George E. Gehrels and Peter G. DeCelles

Department of Geosciences, University of Arizona, Tucson, AZ, USA

ABSTRACT

Sedimentary strata in the Lhasa terrane of southern Tibet record a long but poorly constrained history of basin formation and inversion. To investigate these events, we sampled Palaeozoic and Mesozoic sedimentary rocks in the Lhasa terrane for detrital zircon uranium–lead (U–Pb) analysis. The > 700 detrital zircon U–Pb ages reported in this paper provide the first significant detrital zircon data set from the Lhasa terrane and shed new light on the tectonic and depositional history of the region. Collectively, the dominant detrital zircon age populations within these rocks are 100–150, 500–600 and 1000–1400 Ma. Sedimentary strata near Nam Co in central Lhasa are mapped as Lower Cretaceous but detrital zircons with ages younger than 400 Ma are conspicuously absent. The detrital zircon age distribution and other sedimentological evidence suggest that these strata are likely Carboniferous in age, which requires the existence of a previously unrecognized fault or unconformity. Lower Jurassic strata exposed within the Bangong suture between the Lhasa and Qiangtang terranes contain populations of detrital zircons with ages between 200 and 500 Ma and 1700 and 2000 Ma. These populations differ from the detrital zircon ages of samples collected in the Lhasa terrane and suggest a unique source area. The Upper Cretaceous Takena Formation contains zircon populations with ages between 100 and 160 Ma, 500 and 600 Ma and 1000 and 1400 Ma. Detrital zircon ages from these strata suggest that several distinct fluvial systems occupied the southern portion of the Lhasa terrane during the Late Cretaceous and that deposition in the basin ceased before 70 Ma. Carboniferous strata exposed within the Lhasa terrane likely served as source rocks for sediments deposited during Cretaceous time. Similarities between the lithologies and detrital zircon age-probability plots of Carboniferous rocks in the Lhasa and Qiangtang terranes and Tethyan strata in the Himalaya suggest that these areas were located proximal to one another within Gondwanaland. U–Pb ages of detrital zircons from our samples and differences between the geographic distribution of igneous rocks within the Tibetan plateau suggest that it is possible to discriminate a southern vs. northern provenance signature using detrital zircon age populations.

INTRODUCTION

The Tibetan plateau is the largest region of elevated topography on Earth and forms the basis for much of our understanding of continental deformation and collisional plate tectonics. With respect to its lithosphere-scale structure, the Tibetan plateau is an amalgam of several continental terranes (Fig. 1), which rifted from the northern margin of Gondwanaland during the Palaeozoic and Mesozoic, migrated northward and accreted to southern Asia (Fig. 2; Burg *et al*., 1983; Allégre *et al*., 1984; Dewey *et al*., 1988; Sengör & Nata'lin, 1996; Yin & Harrison, 2000). The southernmost of these continental fragments, the Lhasa terrane, accreted onto southern Asia during the Late Jurassic–Early Cretaceous time (Allégre *et al*., 1984; Dewey *et al*., 1988; Yin & Harrison, 2000). Although the assembly of Tibetan Eurasia implies that significant tectonic activity occurred in the area before the Indo-Asian collision, the style and extent of the deformation and the influence it has had on the subsequent evolution of the Tibetan plateau remain poorly understood.

Much of the geology of Tibet is known only at a cursory or exploratory level. Thus, many basic questions remain unanswered and competing hypotheses are difficult to evaluate because of insufficient data. The Jurassic–Cretaceous history of the Lhasa terrane of southern Tibet provides a prime example of an important but still puzzling stage in the development of the Tibetan plateau. Whereas some argue that southern Tibet had a thickened crust and elevated topography by Cretaceous time (Burg *et al*., 1983; England & Searle, 1986; Pan, 1993; Ratschbacher *et al*., 1993; Murphy *et al*., 1997; Kapp *et al*., 2003a, 2005), others postulate that the region was generally below sea level and characterized by a thinned continental crust during this period

Correspondence: Andrew L. Leier, Department of Geosciences, Princeton University, Princeton, NJ 08544, USA. E-mail: aleier@princeton.edu

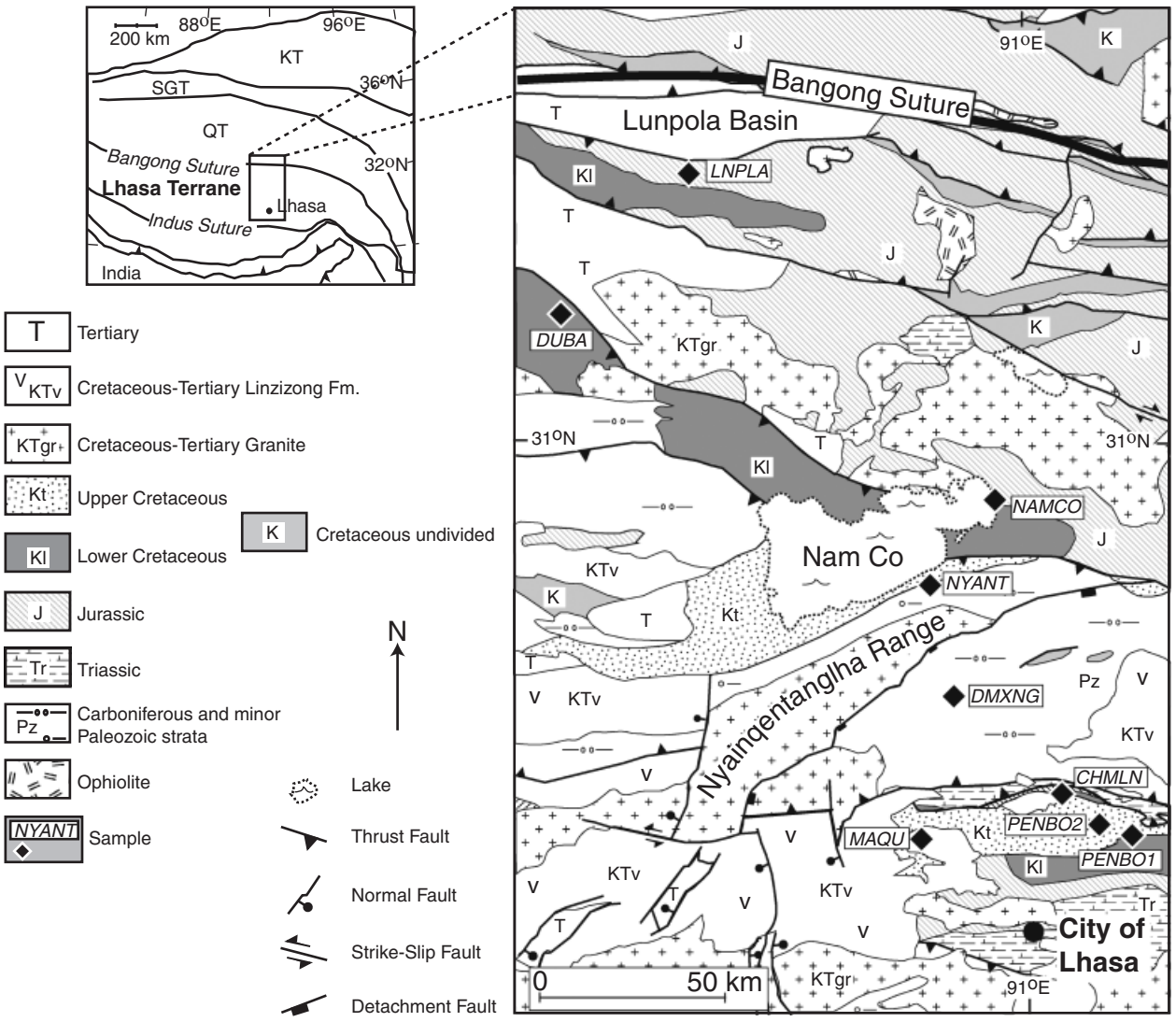

Fig. 1. Simplified geologic map of the study area, central-southern Tibet (modified from Kidd *et al*., 1988). Nine samples were collected from sandstone units exposed in the Lhasa terrane of southern Tibet. In the regional map, KT, Kunlun terrane; SGT, Songpan Ganzi Terrane; QT, Qiangtang terrane.

(e.g. Zhang, 2000; Zhang *et al*., 2004). That such disparate ideas currently coexist is disconcerting, given that the state and nature of southern Tibetan crust just before the collision must be reasonably well constrained before we can accurately reconstruct the processes and products of the Indo-Asian collision.

Basic geochronological and sedimentological data from the sedimentary rocks of the Lhasa terrane are required in order to build reasonable models for the pre-collisional state of southern Asia. In an effort to fill the data gap, we sampled nine sandstone units exposed in the Lhasa terrane (Fig. 1) and determined the uranium–lead (U–Pb) ages of their detrital zircons using laser-ablation multi-collector inductively coupled plasma mass spectrometry (LA-MC-ICPMS). The samples were collected from stratigraphic sections that were measured in detail, and additional samples were taken for analyses of sandstone petrography and provenance.

This investigation was undertaken with the purpose of accomplishing four primary goals, each of which contributes to our understanding of the geologic history of Tibet. The first goal is to obtain maximum depositional ages for stratigraphic units in the Lhasa terrane. Much of the strata in the Lhasa terrane have not been studied in detail. Depositional ages of particular rock units are often speculative, especially when they lack biostratigraphic constraints, which is the case with many units in southern Tibet. Correctly determining the ages of stratigraphic units is necessary for identifying crustal deformation in the region and for constraining depositional basin histories. The second goal is to determine the provenance of sedimentary strata and to reconstruct regional palaeogeographies. The ability to reconstruct the palaeogeography of the Lhasa terrane is a crucial step in constraining the timing, location and style of tectonism in the region, particularly with respect to questions concerning the regional Jurassic–Cretaceous history. The third goal relates to developing a better understanding of the Palaeozoic history of the Lhasa terrane. Comparisons of pre-Mesozoic

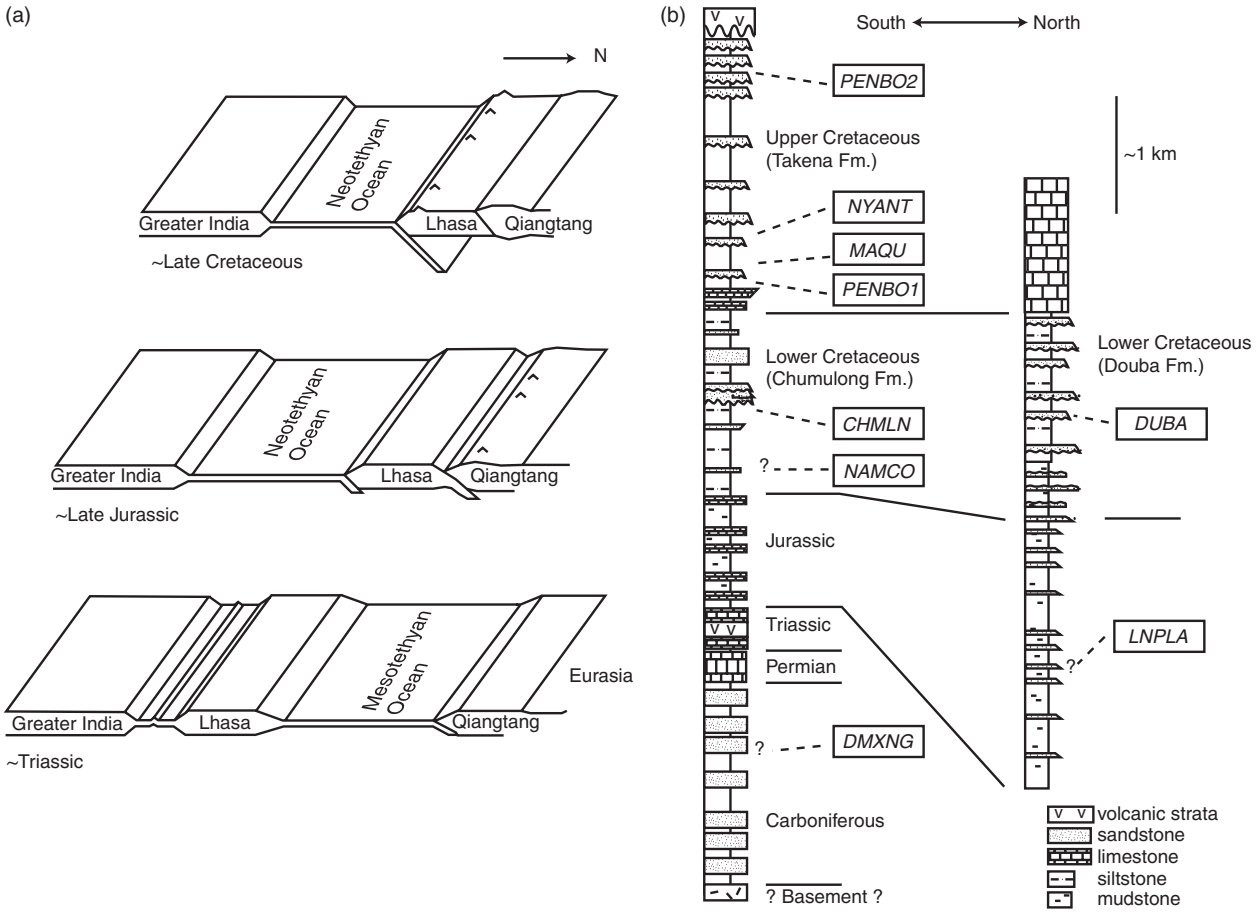

Fig. 2. Tectonic histories of southern Tibet and regional stratigraphy within the Lhasa terrane. (a) Simplified diagrams depicting the assembly of Tibetan plateau terranes. The Lhasa terrane rifted from Greater India (Gondwanaland) during Triassic time and migrated northward. During Late Jurassic–Early Cretaceous time, the Lhasa terrane collided with the Qiangtang terrane. As India moved northward, the Neotethyan oceanic crust was subducted northward beneath the Lhasa terrane. Not to scale. Modified from Yin & Harrison (2000). (b) Regional stratigraphy, including the stratigraphic position of the collected samples. Stratigraphy modified from Yin *et al*. (1988).

detrital zircon populations within the samples allow for the examination of the Palaeozoic relationship between the Lhasa terrane and surrounding tectono-stratigraphic regions of Eurasia. The fourth goal is to provide the foundations for a database that can serve as a point of departure for subsequent studies. The >700 U–Pb ages presented here raise additional questions about the evolution of the Tibetan plateau and can be utilized in future geological investigations of Tibet.

GEOLOGIC FRAMEWORK

Tectonic evolution

The Lhasa terrane was a constituent of Gondwanaland and located in the southern hemisphere throughout most of the Palaeozoic (Dewey *et al*., 1988; Sengör & Nata'lin, 1996; Yin & Harrison, 2000). The Indian portion of Gondwanaland experienced partial break-up during late Palaeozoic time as individual terranes such as the Qiangtang and Lhasa terranes rifted from the northern margin of India and migrated northward (Dewey *et al*., 1988; Sengör & Nata'lin, 1996; Yin & Harrison, 2000; Stampfli & Borel, 2004). The collision between the Lhasa and Qiangtang terranes occurred during latest Jurassic–earliest Cretaceous time along the Bangong suture (Figs 1 and 2; Kidd *et al*., 1988; Liu, 1988), and resulted in a collisional orogen and the formation of a peripheral foreland basin within the northern part of the Lhasa terrane (Dewey *et al*., 1988; Leeder *et al*., 1988; Murphy *et al*., 1997; Kapp *et al*., 2005). The peripheral foreland basin persisted into the Early Cretaceous (Leeder *et al*., 1988; Murphy *et al*., 1997; Zhang *et al*., 2004) and was in some locations overprinted by volcanism associated with north-dipping subduction of Neotethyan oceanic crust beneath the Lhasa terrane (Allégre *et al*., 1984; Coulon *et al*., 1986; Kapp *et al*., 2005). Continued subduction of Neotethyan crust along the southern margin of the Lhasa terrane ultimately produced the Gangdese volcanic arc (Fig. 2; Allégre *et al*., 1984; Dewey *et al*., 1988). Structural evidence suggests that the crust of southern Tibet was roughly twice the normal thickness by the end of

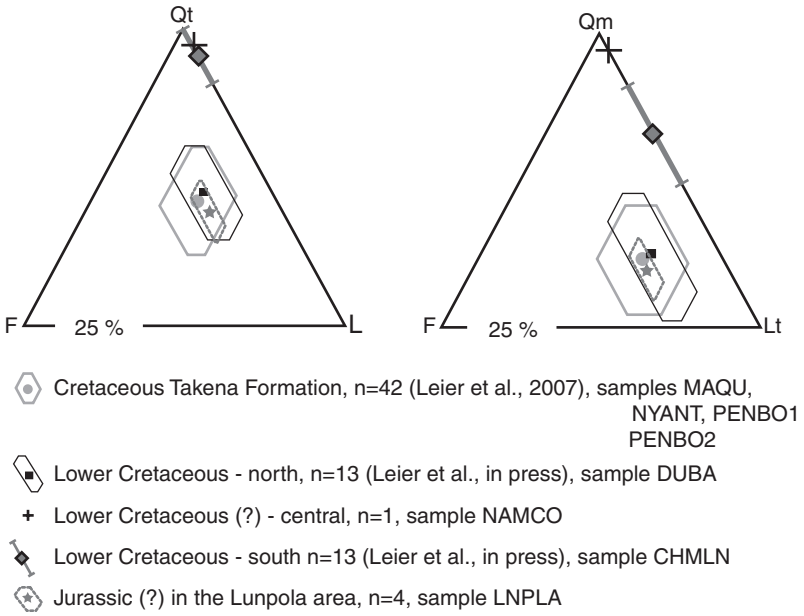

Fig. 3. Sandstone petrography of the strata associated with the collected samples. Qt, total quartz; F, feldspar; L, lithics; Qm, monocrystalline quartz; Lt, total lithics (including polycrystalline quartz). The data shown include the mean modal composition (the symbol) and 1 SD (the line surrounding the symbol).

Cretaceous time (Burg *et al.*, 1983; England & Searle, 1986; Pan, 1993; Ratschbacher *et al.*, 1993; Murphy *et al.*, 1997; Kapp *et al.*, 2003a, 2005).

Stratigraphy

Palaeozoic sedimentary strata in the Lhasa terrane consist primarily of Carboniferous sandstone, metasandstone, shale and phyllite, and lesser Ordovician, Silurian and Permian limestone (Fig. 2; Leeder *et al.*, 1988; Liu, 1988; Yin *et al.*, 1988). Exposures of Precambrian strata are rare but have been reported in Hu *et al.* (2005). Triassic rocks include inter-bedded limestone and basaltic volcanic units, which are most prevalent along the southern margin of the terrane (Leeder *et al.*, 1988). Jurassic strata in the northern Lhasa terrane consist of deepwater sandstone and shale, and in many places are associated with ophiolitic assemblages (Leeder *et al.*, 1988; Yin *et al.*, 1988). Jurassic deposits in the southern half of the terrane are composed of marine limestone and mudstone (Yin *et al.*, 1988). Lower Cretaceous strata consist of clastic mudstone, sandstone and local conglomerate units (Yin *et al.*, 1988). Overlying the Lower Cretaceous clastic units is a widely exposed shallow marine limestone of Aptian–Albian age (Yin *et al.*, 1988; Liu, 1988), which, in some locations, also contains fossils of Cenomanian age (Zhang, 2000). Upper Cretaceous strata in the Lhasa terrane consist of arkosic fluvial sandstone and mudstone successions (Fig. 2; Leier *et al.*, in press).

SAMPLES

Sandstone samples were collected from exposures of Phanerozoic strata in the Lhasa terrane (Fig. 1). In addition to being prepared for detrital zircon geochronology (see 'Methods'), standard petrographic thin sections were cut, stained for potassium feldspar and calcic plagioclase and point-counted (450 counts slide^{-1}) using a modified Gazzi–Dickinson method (Ingersoll *et al.*, 1984); counting parameters and recalculated detrital modes can be accessed in the auxiliary material (Table S1). Brief descriptions of the sampled strata are presented below along with modal compositions (Qm, monocrystalline quartz; Qt, total quartz; F, feldspar; L, non-quartzose lithic grains; Lt, total lithic grains including quartzose fragments), which are also shown in Fig. 3.

Carboniferous strata

Carboniferous strata comprise a significant proportion (> 50%) of the Phanerozoic sedimentary sequence in the Lhasa terrane and are widely exposed in southern Tibet (Fig. 1; Yin *et al.*, 1988; Liu, 1988). Sample DMXNG is from a Carboniferous quartzose sandstone exposed southeast of the Nyainqentanglha range (Figs 1 and 2). Sedimentary strata of Carboniferous age were deposited under marine conditions and locally contain glaciomarine deposits (Leeder *et al.*, 1988; Yin *et al.*, 1988).

Jurassic(?) strata

Sample LNPLA is a medium- to coarse-grained sandstone collected from a succession of Jurassic(?) sedimentary rocks exposed along the southern margin of the Lunpola basin, near the Bangong suture (Figs 1 and 2). The sandstone beds were deposited by submarine turbidity currents within a marine basin that was located south of the Qiangtang terrane and north of the Lhasa terrane (Fig. 2; Leeder *et al.*, 1988; A. L. Leier, unpublished data). The

strata are lithic-rich and have an average modal composition of Qm/F/Lt = 49/16/35, and Qt/F/L = 62/16/22 (Fig. 3). Volcanic grains of intermediate to mafic composition, and commonly with laths of plagioclase, constitute the most abundant type of lithic grain. Chlorite, serpentine and pyroxene are common accessory minerals.

Lower Cretaceous strata – north

Sample DUBA was collected from a medium-grained fluvial sandstone unit of the Lower Cretaceous Duoba Formation, which is exposed approximately 50 km south of the LNPLA sample site (Figs 1 and 2). The Lower Cretaceous Duoba Formation is >1300 m thick and composed primarily of fluvial sandstone and pebble-conglomerate beds inter-stratified with floodplain mudstone (Leeder *et al*., 1988; Leier *et al*., in press). The modal composition of the sandstone in the Duoba Formation is Qm/F/Lt = 42/16/42 and Qt/F/L = 57/16/27 (Fig. 3; Leier *et al*., in press), with the majority of the lithic population composed of felsic volcanic grains. Although questions remain about the specific tectonic setting and sedimentary provenance of these strata (cf. Leeder *et al*., 1988; Murphy *et al*., 1997; Zhang *et al*., 2004), palaeocurrent data uniformly record southwest-directed sediment transport (i.e. north-northeastward source area; Leeder *et al*., 1988).

Lower Cretaceous strata – central

Sample NAMCO was collected from buff-coloured, Lower Cretaceous(?) sandstone exposed along the northeastern shore of the lake Nam Co (Figs 1 and 2). Sandstone within the succession is quartzose with modal compositions of Qm/F/Lt = 95/0/5, and Qt/F/L = 96/0/4 (Fig. 3), thin to thickly bedded, contains symmetrical ripples and is commonly inter-bedded with mudstone and siltstone. These strata are extensively folded and faulted at the outcrop scale (~100–1000 m).

Lower Cretaceous strata – south

Sample CHMLN was collected from the Lower Cretaceous Chumulong Formation (Yin *et al*., 1988) in the southern half of the Lhasa terrane (Figs 1 and 2). The Chumulong Formation contains inter-bedded sandstone, mudstone and local quartzite pebble-conglomerate, all of which were deposited in marginal marine and fluvial environments (Leier *et al*., in press). Sandstone units within the Lower Cretaceous succession are typically quartz-rich with an average modal composition of Qm/F/Lt = 73/0/27 and Qt/F/L = 92/0/8 (Fig. 3); zircon is the primary accessory mineral (Leier *et al*., in press).

Upper Cretaceous Strata

Four samples were collected from medium-grained fluvial sandstone beds of the Upper Cretaceous Takena Formation. Specific sampling locations of the Takena Formation include the Maqu area northwest of Lhasa (sample MAQU), the Penbo area northeast of the city of Lhasa (two samples, PENBO1 and PENBO2), and from the Nyainqentanglha range south of Nam Co (sample NYANT; Figs 1 and 2). The sandstone beds of the Takena Formation that were sampled are part of a >1.5-km-thick succession of clastic fluvial lithofacies that were deposited by northwestward-flowing rivers in a Cretaceous retro-arc foreland basin (Burg *et al*., 1983; England & Searle, 1986; Leier *et al*., 2007). Sandstone units within the Takena Formation contain abundant plagioclase and volcanic grains and have average modal compositions of Qm/F/Lt = 41/18/41 and Qt/F/L = 56/18/26 (Fig. 3; Leier *et al*., 2007).

METHODS

Detrital zircons were extracted from the nine samples (~15 kg/sample) at the University of Arizona following the procedures outlined in Gehrels (2000). Once separated, the detrital zircons were encased in epoxy within 1 in. ring mounts, which were then sanded and polished to produce a smooth flat surface that exposed the interiors of the zircon grains. One-hundred individual zircon grains were analysed from each sample. These were selected randomly from all sizes and shapes, although grains with obvious cracks or inclusions were avoided.

U–Pb ages of detrital zircons were obtained using an LA-MC-ICP-MS (GVI Isoprobe; GV Instruments, Manchester, UK). The interiors of the zircon grains were ablated using a New Wave DUV193 Excimer laser (New Wave Instruments, Provo, UT, USA and Lambda Physik Inc., Ft Lauderdale, FL, USA) operating at a wavelength of 193 nm and using a spot diameter of 35–50 μm; laser ablation pits are ~20 μm deep. With the LA-MC-ICP-MS, the ablated material is carried via argon gas to the plasma source of a Micromass Isoprobe, which is configured in such a way that U and Pb can be measured simultaneously. Measurements are made in the static mode using Faraday collectors for ^{238}U, ^{232}Th, ^{208}Pb, ^{207}Pb, ^{206}Pb and an ion-counting channel for ^{204}Pb. Analyses consist of one 20 s integration with the peak centred but no laser firing (checking background levels), and 20 1 s integrations with the laser firing on the zircon grain. At the end of each analysis, a 30-s delay occurs during which time the previous sample is purged from the system and the peak signal intensity returns to background levels. The contribution of Hg to the ^{204}Pb is accounted for by subtracting the background values. Common lead corrections are made using the measured ^{204}Pb of the sample and assuming initial Pb compositions from Stacey & Kramers (1975). A fragment of a zircon crystal of known age (564 ± 4 Ma, 2σ error; G. E. Gehrels, unpublished data) is analysed after every fifth zircon analysis to correct for inter-element and Pb isotope fractionation. The ages presented are $^{206}Pb^*/^{238}U$ ages for grains less than ~1000 Ma and $^{207}Pb^*/^{206}Pb^*$ ages for grains with ages >1000 Ma. All uncertainties of individual grains are reported at the 1 σ level and include only measurement errors; systematic errors would increase age uncertainties by 1–2%. Those analyses with >10% uncertainty ($^{206}Pb^*/^{238}U$ ages) or more than

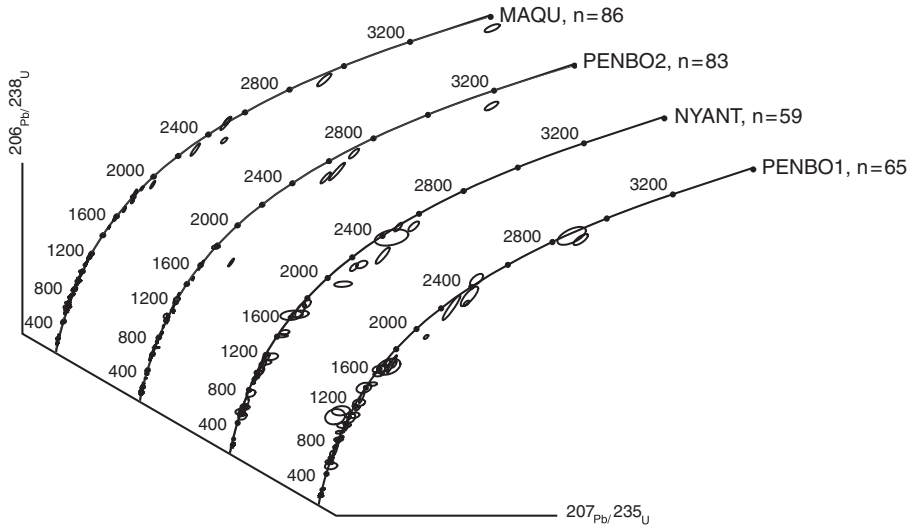

Fig. 4. Concordia diagram of the samples collected from the Upper Cretaceous Takena Formation. Ages are in Ma and ellipses show 2σ errors. The name of the individual sample and the number of zircons that were sufficiently concordant to be used in the study can be noted next to the concordia curve.

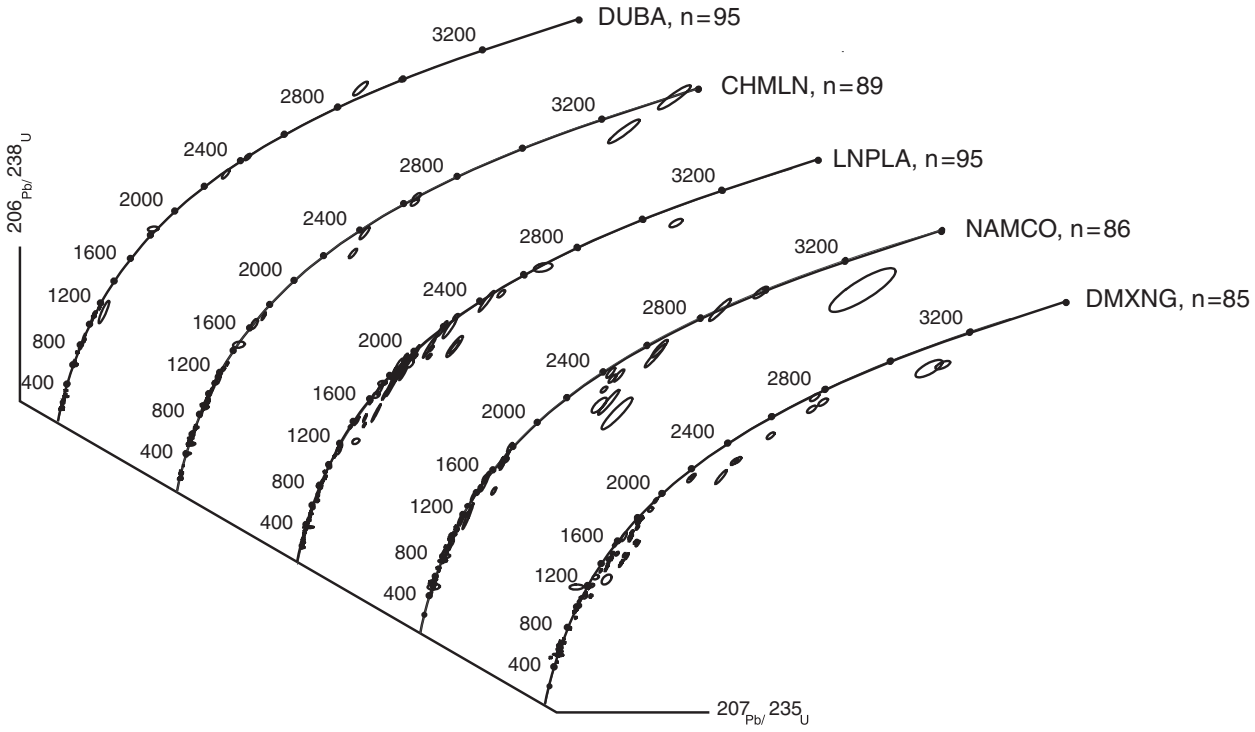

Fig. 5. Concordia diagram of samples collected from the Lhasa terrane, excluding the Upper Cretaceous samples. Ages are in Ma and ellipses show 2σ errors. The name of the individual sample and the number of zircons that were of sufficient concordance to be used in the study can be noted next to the concordia curve.

20% discordance or 5% reverse discordance are omitted from further consideration. The data from each sample are displayed on concordia diagrams and age–probability plots/histograms using the programs of Ludwig (2001). Age–probability plots depict each age and its uncertainty as a normal distribution, summing all ages from the analysed zircons of a sample into one curve, which is then divided by the total number of analysed zircons. Maximum depositional ages are calculated from the weighted mean of the youngest cluster with three or more overlapping ages; uncertainties reported with the maximum depositional ages include both the measurement and systematic errors.

RESULTS

In the following paragraphs and in Figs 4–7, we present the most salient features of each sample (see also Supplementary Table S1). Interpretations and implications of the data

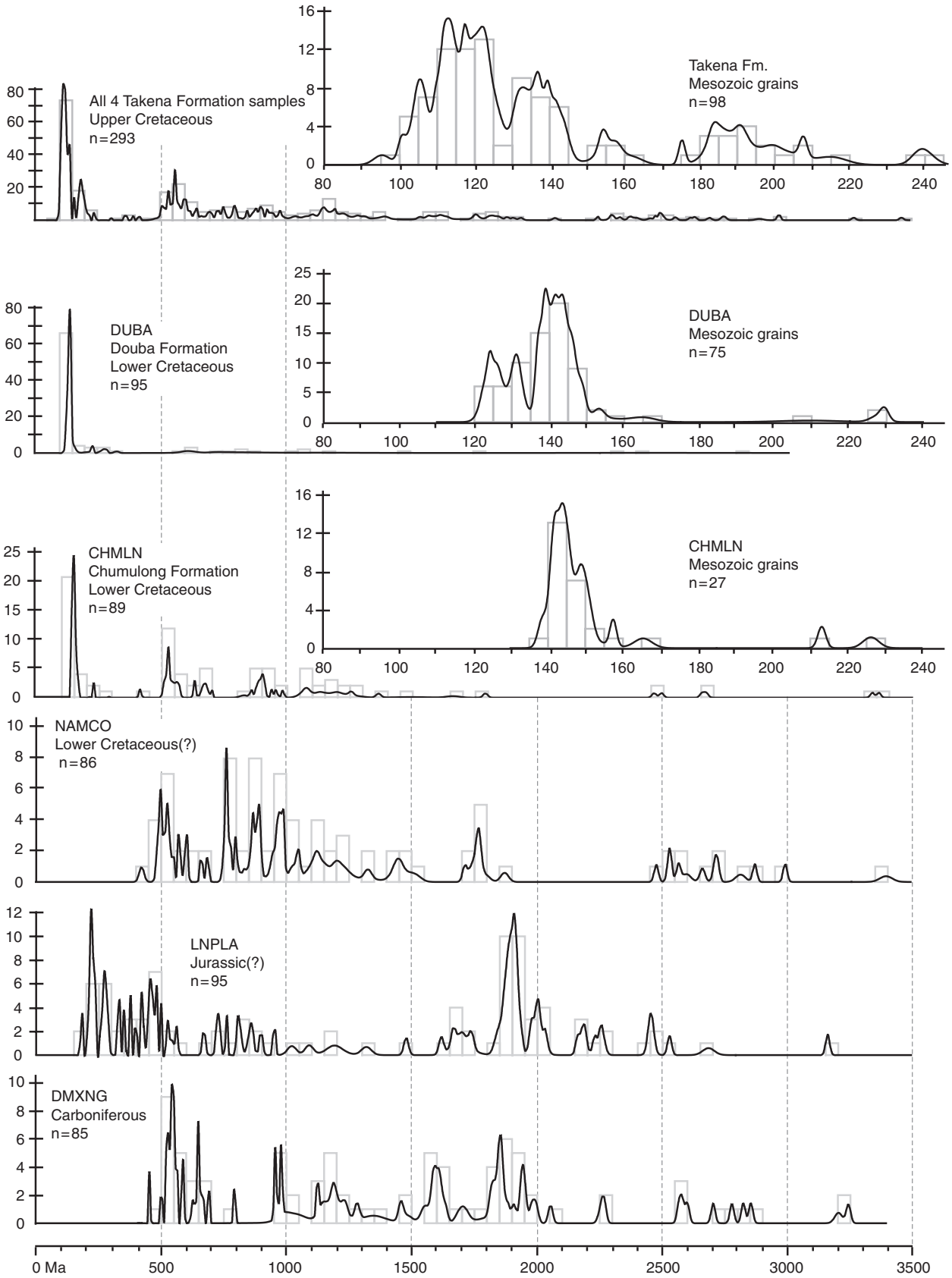

Fig. 6. Relative probability plots and histograms of detrital zircon uranium–lead ages. All four of the samples from the Upper Cretaceous Takena Formation have been combined into one curve. The number of zircons (histogram) is given on the vertical axis; the age, in Ma, is on the horizontal axis. Bin size for the histogram is 50 Myr. Insets with the samples of Cretaceous strata show distribution of zircons of Mesozoic age; the bin size for the Mesozoic populations is 5 Myr. Although sample NAMCO is mapped as Lower Cretaceous, it did not contain detrital zircons with ages < 400 Ma. See text for complete discussion of the data.

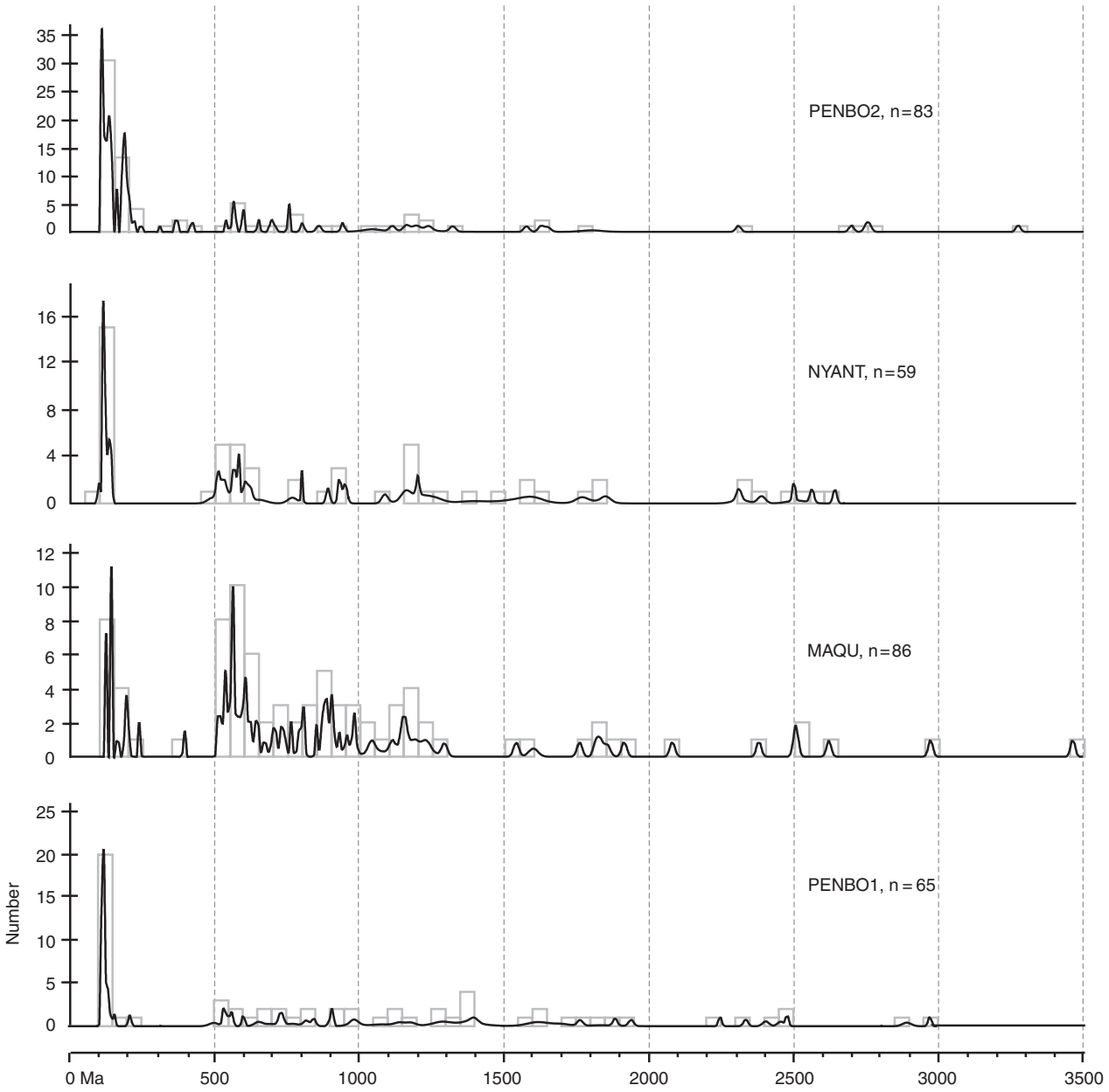

Fig. 7. Relative probability plots and histograms of detrital zircon uranium–lead ages from the Upper Cretaceous samples. The number of zircons (histogram) is given on the vertical axis; the age, in Ma, is on the horizontal axis. The bin size for the histogram is 50 Myr.

are discussed in the following section. All period and epoch-to-age correlations are based on the time scale compiled by Palmer & Geissman (1999).

Carboniferous strata

Sample DMXNG yielded 85 usable ages (Figs 5 and 6). The youngest cluster of zircons has a mean age of 548 ± 9 Ma, although a few individual zircon grains with younger ages (~455 Ma) are also present. The largest population of detrital zircons is within the 500–600 Ma range (peak at 540 Ma), with additional populations in the ranges of 1050–1300 Ma (peak at 1120 Ma), 1700–1950 Ma (peak at 1850 Ma) and some scattered ages around 2500 Ma.

Jurassic(?) strata

Sample LNPLA yielded 95 usable ages (Figs 5 and 6). The majority of the zircons are medium-grained (size varies from fine to coarse grained) and angular (euhedral to subhedral). The most robust maximum depositional age for these strata is 270 ± 6 Ma (based on four zircons). However, nine of the 95 zircons yielded ages between 179 and 260 Ma, including a pair that has a mean age of 179 ± 6 Ma, suggesting that the strata may be younger than 270 Ma (see 'Discussion'). The largest cluster of detrital zircons is between 1850 and 2050 Ma (peak at ~1900 Ma), and a fairly large population of detrital zircons with ages between 200 and 500 Ma is also present.

Lower Cretaceous strata – north

Sample DUBA yielded 95 usable ages (Figs 5 and 6). The zircons are almost entirely medium to coarse grained and very angular (euhedral). The youngest cluster of ages has a mean of 125 ± 2 Ma, which provides a maximum depositional age for the Duoba Formation. Zircon grains with ages between 125 and 150 Ma are by far the most numerous (peak at 140 Ma), representing over 65% of all the detrital zircon ages. Zircons with ages older than 150 Ma are few, but those that are present have ages of 250–340, 610–670, 700–900 and 1000–1200 Ma. Zircons yielding ages > 150 Ma tend to be subrounded to rounded (anhedral) and spherical.

Lower Cretaceous Strata – Central

Sample NAMCO yielded 86 usable ages (Figs 5 and 6). The zircons are typically fine to medium grained and rounded but the morphologies vary between subangular and well rounded (subhedral to anhedral). The youngest cluster of ages constrains the maximum depositional age at 495 ± 8 Ma; of the zircons analysed, not a single grain yielded an age < 400 Ma. Similar to many of the other samples, a significant proportion of the detrital zircons have ages between 500 and 600 Ma. Zircons with ages of 750–1000 Ma have peaks at ~760, 890 and 970 Ma. Also within the sample, detrital zircons with ages between 1000 and 1400 Ma (peak at 1150 Ma) are present, as are small populations between 1700 and 1800 Ma and between 2500 and 3000 Ma.

Lower Cretaceous strata – south

Sample CHMLN yielded 89 usable ages (Figs 5 and 6). Zircons vary from fine to medium grained and are angular to rounded (euhedral to anhedral). The maximum depositional age is 143 ± 2 Ma, corresponding to Early Cretaceous time. The largest population of zircons in this sample has ages between 140 and 150 Ma, the second largest having ages between 500 and 600 Ma. The Lower Cretaceous deposits in the Penbo area have a significant number ($n = 15$) of Middle Proterozoic zircons with ages between 1000 and 1400 Ma but very few with ages > 1500 Ma. Generally, zircons with ages > 150 Ma are more rounded than their younger counterparts, although there are several exceptions to this.

Upper Cretaceous strata

Together, the four samples from the Takena Formation yielded 293 usable (Figs 4, 6 and 7). The zircons vary from fine to coarse grained and have very angular to well-rounded morphologies (euhedral to anhedral). The youngest cluster of ages is between 100 and 105 Ma, and is from a fluvial sandstone within the uppermost portion of the Takena Formation (sample PENBO2; Fig. 7). Zircons of Cretaceous age comprise the largest population, with ages generally between 105 and 140 Ma (peak at 120 Ma). Early Jurassic zircons with ages between 180 and 200 Ma (peak at 190 Ma) form a subordinate group within the Mesozoic population. Outside of the Mesozoic-age population, the second-largest number of zircons has ages between 500 and 600 Ma (peak at ~550 Ma). Each of the samples contains at least a few zircons with ages between 650 and 1000 Ma, which are evenly distributed across this age interval. A significant proportion of zircons within the Takena Formation samples have ages of 1000–1400 Ma (peak at ~1150 Ma) and there is commonly a scattered group centred at ~2500 Ma. As with the other samples, zircons with ages > 500 Ma are typically more rounded than the younger zircons but this is not always the case.

Comparison of ages

Many of the sandstone samples collected from the Lhasa terrane have similar populations of detrital zircons (Fig. 6). All Cretaceous sandstone samples (CHMLNG, MAQU, PENBO1, PENBO2, NYANT) contain numerous zircons with ages between 110 and 160 Ma, with smaller subclusters at ~120 and ~140 Ma. The Cretaceous(?) NAMCO sample collected near Nam Co is a notable exception to this trend, and in fact, lacks any zircons with ages < 400 Ma (Fig. 6). Except for detrital zircons from the Jurassic sandstone exposed near the Bangong suture (sample LNPLA), zircons with ages between 200 and 500 Ma are scarce (Fig. 6). In contrast, detrital zircons with 500–600 Ma ages typically represent a substantial proportion of the total population in many of the samples. All samples contain at least a few zircons with ages between 650 and 950 Ma, although it is difficult to discern a common peak within this range. Many of the samples contain a significant population of zircons with ages of 1000–1400 Ma (peak at ~1150 Ma). With the exception of the LNPLA sample, the samples typically contain only a small number of detrital zircons with ages between 1500 and 2000 Ma; the Jurassic LNPLA sample contains a conspicuously large cluster at ~1900 Ma (Fig. 6). Almost all the samples contain a small number of zircons with ages ~2500 Ma.

DISCUSSION

'Lower Cretaceous' strata at Nam Co

Sandstone exposed along the northeastern shore of Nam Co (sample NAMCO; Fig. 1) has been mapped as Lower Cretaceous (e.g. Liu, 1988), but the absence of grains < 400 Ma suggest that this designation may be incorrect. Lower Cretaceous strata to the south and north of Nam Co are dominated by detrital zircons of Early Cretaceous age (e.g. samples CHMLNG and DUBA; Fig. 6) and the ages of plutonic and volcanic rocks proximal to the Nam Co sampling site indicate that there was abundant Early Cretaceous volcanism in the area (e.g. Coulon *et al.*, 1986; Kapp, *et al.*, 2005). This raises the question as to why not a single zircon from the NAMCO sample has an Early Cretaceous age. The anhedral morphology of the

zircons suggests that they are recycled grains (Fig. 8), but this does not explain the absence of younger zircons. Other samples of Cretaceous strata contain similar anhedral zircon grains but they also contain zircons with ages between 150 and 400 Ma. The sandstone composition of the strata in question and the degree of deformation are also anomalous relative to Lower Cretaceous strata exposed to the north and west of the area (e.g. sample DUBA; Fig. 1).

The most plausible explanation for the anomalous detrital zircon ages from sample NAMCO is that the strata exposed along the northeastern margin of Nam Co are Palaeozoic in age, and not Lower Cretaceous; similarities between the lithology and detrital zircon age distribution of the strata northeast of Nam Co to those of Carboniferous rocks elsewhere in the region suggest that the strata near Nam Co are most likely Carboniferous in age. If these strata are indeed Carboniferous in age, this discovery will have important implications for understanding upper crustal deformation in the central Lhasa terrane. In order to account for the juxtaposition of Palaeozoic strata with Cretaceous rocks (Fig. 1), a previously unrecognized fault or major unconformity would have to exist in the area northeast of Nam Co. Regardless of whether this relationship is fault or unconformity related, the presence of Palaeozoic strata at the surface will require a reinterpretation of the upper crustal structure in the central Lhasa terrane.

Jurassic strata

Recent studies suggest that the Jurassic–Cretaceous collision between the Lhasa and Qiangtang terranes was one of the most significant tectonic events to have occurred in southern Asia before the Indo-Asian collision (Fig. 2; e.g. Leeder *et al.*, 1988; Murphy *et al.*, 1997; Arnaud *et al.*, 2003; Kapp *et al.*, 2005; Guynn *et al.*, 2006); however, many aspects of this event are poorly understood. The northward movement of the Lhasa terrane before the collision was accommodated by subduction of Mesotethyan oceanic crust beneath the Qiangtang terrane, which ultimately should have produced a magmatic arc along the southern margin of the Qiangtang terrane (Fig. 2; e.g. Guynn *et al.*, 2006). The paucity of evidence for a Jurassic-age magmatic arc along the southern margin of the Qiangtang terrane raises questions about the validity of this tectonic reconstruction.

The Jurassic strata exposed near the Bangong suture (sample LNPLA) were deposited in a basin located between the Lhasa and Qiangtang terranes sometime before the Lhasa–Qiangtang collision (Leeder *et al.*, 1988; Yin *et al.* 1988). The small number of detrital zircons of Jurassic age within the LNPLA sample ($n < 5$) can be interpreted in several ways. If the Jurassic strata were derived from the southern margin of the Qiangtang terrane (e.g. Leeder *et al.*, 1988), it is difficult to reconcile the small number of Jurassic-age zircons within the sample with the existence of a robust magmatic arc in the Qiangtang terrane. Thus, the detrital zircon ages within this succession may be used as evidence against the former existence of a Jurassic magmatic arc along the southern margin of the Qiangtang terrane. However, other factors must first be considered before such an inference can be made. The ages of the detrital zircons in the LNPLA sample indicate a maximum depositional age of 270 ± 6 Ma, or a more tentative 179 ± 6 Ma. If the more robust 270 Ma age is used as a reasonable proxy for the depositional age, it is possible that these strata were deposited during Permo-Triassic time, which would mean the strata are not associated with the Lhasa-Qiangtang collision and the closure of the Mesotethyan ocean; rather, these rocks would be associated with the preceding rifting of the Qiangtang terrane from northern Gondwanaland (i.e. the Lhasa terrane) and the formation of the Mesotethyan ocean. Furthermore, the primary period of igneous activity in the southern Qiangtang terrane is thought to have been between 180 and 170 Ma (Guynn *et al.*, 2006). Therefore, even if the more questionable age of 179 ± 6 Ma is used as a proxy for depositional age, deposition of the sediment associated with these strata may have predated the formation of a Qiangtang magmatic arc, which would explain why so few detrital zircons of Jurassic age are present in the unit. The abundance of mafic volcanic grains within the strata are equivocal and can be used to argue for deposition during a rifting-related phase, and hence an older depositional age associated with formation of the Mesotethyan ocean, or deposition during a contraction-related phase associated with closure of the Mesotethyan ocean, and therefore a younger depositional age. As it currently stands, all these scenarios can only be speculated upon and further investigation is needed before the full meaning and importance of these sedimentary rocks can be determined.

Upper Cretaceous strata

Determining the tectonic setting of southern Tibet just before the Indo-Asian collision (i.e. Late Cretaceous) is important because variations in properties such as initial crustal thickness or surface elevation can play a large role in controlling how the southern margin of the Eurasian plate responded to the subsequent collision with India (e.g. England & Houseman, 1986). The most complete record of this time period is preserved in the Upper Cretaceous Takena Formation; however, a major obstacle to using these strata for palaeotectonic and palaeogeographic reconstructions is the lack of detailed provenance information and poor age control. Estimates of the depositional age of the Takena Formation can be resolved only as sometime between $\sim$105 and $\sim$70 Ma based on fossils in underlying limestone beds (Leeder *et al.*, 1988; Leier *et al.*, 2007) and the zircon crystallization age of volcanic rocks that overlie deformed beds of the Takena Formation, respectively (He, 2005).

Because the Takena Formation was deposited proximal to and coeval with abundant Late Cretaceous volcanism and contains volcanic clasts (Leier *et al.*, 2007), detrital zircon U–Pb geochronology may provide one of the few approaches that can be used to better constrain depositional ages. For example, sample PENBO1 was collected

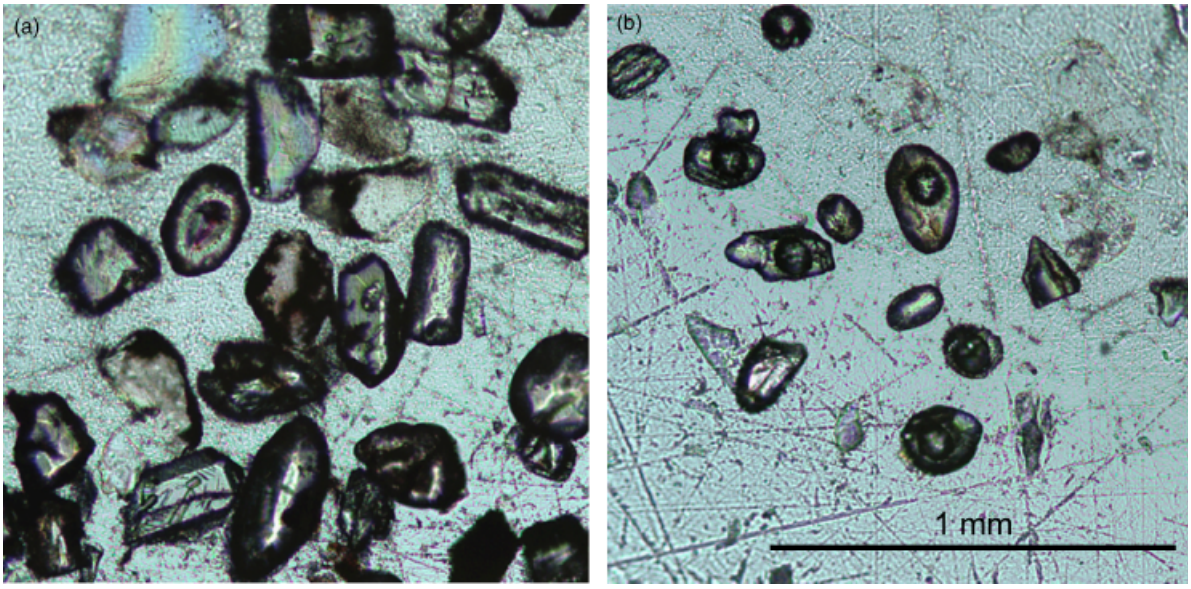

Fig. 8. Photos of the detrital zircon grains. The detrital zircon grains from sample PENBO2 (a) are generally euhedral but vary from euhedral to anhedral, whereas those from sample NAMCO (b) are typically subhedral to anhedral.

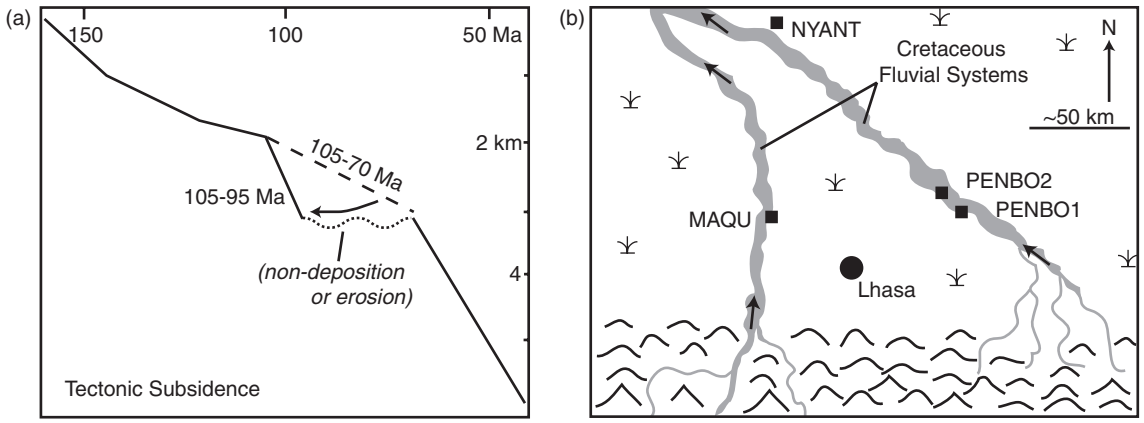

Fig. 9. Applications of detrital zircon data to reconstructions of Late Cretaceous subsidence and palaeogeography. (a) Cretaceous–Tertiary subsidence history of the southern portion of the Lhasa terrane. Detrital zircon ages suggest that deposition of the Upper Cretaceous Takena Formation ceased well before 70 Ma, which increases the subsidence rate in the area during Late Cretaceous time. (b) Palaeogeographic reconstruction of the Late Cretaceous fluvial systems that occupied the southern portion of the Lhasa terrane; approximate sample localities and modern site of the city of Lhasa are shown for reference. Arrows indicate approximate palaeocurrent directions. Differences in the detrital zircon age population of sandstone at the MAQU site, along with differences in sandstone petrography, indicate that the fluvial system in that location was distinct from the fluvial systems to the north and east.

from a fluvial sandstone bed located ~200 m stratigraphically metres above limestone beds with middle Albian fossils (~105 Ma, based on the time scale of Palmer & Geissman, 1999; Leier *et al.*, 2007). The youngest detrital zircon U–Pb ages from PENBO1 are between 110 and 115 Ma, which suggests that the youngest detrital zircon ages from a sample may be reasonable proxies for depositional ages (± 10 Ma). Significantly, none of the detrital zircons analysed from the Takena Formation is younger than 100 Ma, including those from sample PENBO2 (Fig. 8), which was collected from the uppermost portion of the formation. Although the known age constraints indicate that deposition of the Takena Formation occurred sometime between 105 and 70 Ma, the fact that the youngest detrital zircon ages from the uppermost beds of the Takena Formation are all > 100 Ma suggests that deposition may have ceased well before 70 Ma. The shorter duration of deposition inferred from the detrital zircons from the Takena Formation indicates accelerated subsidence during the Late Cretaceous (Fig. 9a).

During the Late Cretaceous, the southern portion of the Lhasa terrane was characterized by generally north-northwestward-flowing rivers and interfluvial floodplains (Leier *et al.*, 2007). The southern margin of the terrane served as a sediment source and deposition occurred within the central to northern reaches of the Lhasa terrane. The detrital zircon ages from the Takena Formation fluvial sandstones can be used to refine Late Cretaceous

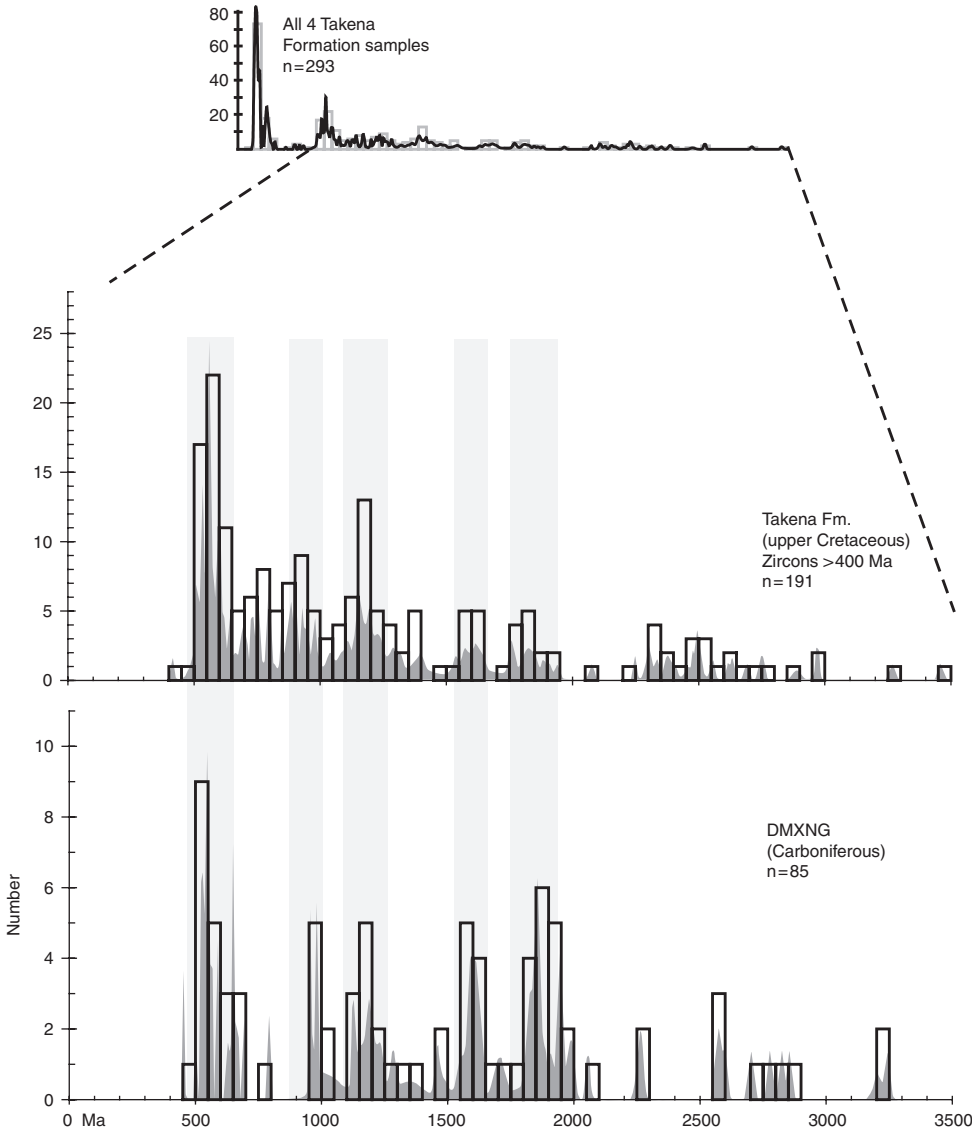

Fig. 10. Diagrams comparing the distribution of detrital zircon uranium–lead ages in samples from the Takena Formation with that from a sample of Carboniferous strata exposed within the Lhasa terrane. Enlarged are the detrital zircons from the Takena Formation that have ages >400 Ma; below this are all the detrital zircon ages from the sample of Carboniferous strata. This figure highlights the fact that the older zircons within the Takena Formation have ages that are very similar to the ages of zircons in the Carboniferous strata. This information, combined with petrographic data and regional map-relationships, suggests that Carboniferous strata were exposed at the surface, eroded and redeposited during the Late Cretaceous.

palaeogeography reconstructions. Compared with the Takena Formation at other sample locations (NYANT, PENBO1 and PENBO2), the MAQU location is characterized by a greater proportion of >500 Ma detrital zircons, and higher percentages of potassium feldspar, metamorphosed lithic grains and tectonized quartz grains. This suggests that the Maqu-area rivers may have drained distinct, more deeply eroded (e.g. Dickinson & Suczek, 1979) source-area basins (Fig. 9b).

Carboniferous strata at the surface during Cretaceous time

Cretaceous strata in the Lhasa terrane contain lithic grains derived from source terranes composed of shale, phyllite, sandstone and quartzite; thus, these deposits were derived at least in part from pre-Cretaceous sedimentary and meta-sedimentary rocks (Leier *et al.*, in press). Carboniferous strata are ideal candidates for source rocks because they are the thickest pre-Cretaceous strata in the Lhasa terrane, they include sedimentary and low-grade meta-sedimentary rocks and are unconformably overlain by Cretaceous strata in some areas (Fig. 1; Liu, 1988; Yin *et al.*, 1988). Figure 10 compares the distribution of >400 Ma detrital zircons from all Takena Formation samples and with the distribution of detrital zircon ages from sample DMXNG, which was collected from a Carboniferous sandstone exposed in the southern Lhasa terrane. The two age distributions are remarkably similar, implying that Carboniferous rocks served as a source for Cretaceous

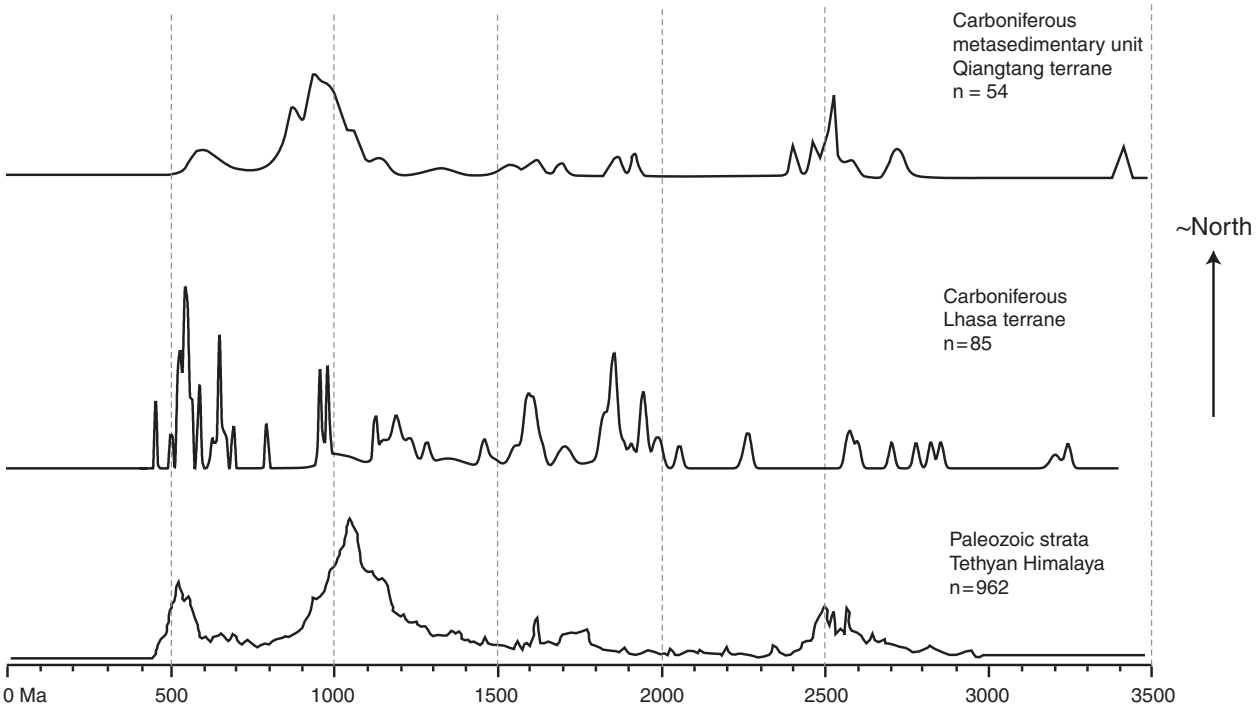

Fig. 11. Comparison of detrital zircon uranium–lead ages from Palaeozoic strata in tectono-sedimentary terranes in the Himalayan–Tibetan orogenic system. The lowermost relative probability curve is from Tethyan Himalayan strata exposed in northern Nepal and southern Tibet (from DeCelles *et al*., 2004). The middle relative probability curve is from Carboniferous strata exposed in the Lhasa terrane; sample DMXNG, this study. The uppermost relative age–probability curve is from Carboniferous metasandstones exposed in the Qiangtang terrane (from Kapp *et al*., 2003a). Although there are some differences, the first-order similarity of detrital zircon ages between samples supports early–middle Palaeozoic plate reconstructions that depict the northern margin of India, the Lhasa terrane, and the Qiangtang terrane as covered by a contiguous marine environment along the northern margin of Gondwanaland.

deposits. Combined with the petrographic evidence and stratigraphic relationships mentioned above, the detrital zircon data indicate that Carboniferous strata were exposed and being eroded during Cretaceous time in southern Tibet. The fact that Carboniferous rocks remain widely exposed in the Lhasa terrane today in turn implies that relatively little post-Cretaceous erosion has occurred in this region.

Palaeozoic strata and northern Gondwanaland

Detrital zircon ages from Palaeozoic sedimentary rocks in southern Tibet can be compared with those from age-equivalent rocks in the Qiangtang terrane to the north and the Himalayan thrust belt of Nepal to the south as a means of evaluating Palaeozoic palaeogeographic models of northern Gondwanaland. Detrital zircon ages from Carboniferous strata in the Lhasa terrane (sample DMXNG) are similar to those from Palaeozoic strata of the Tibetan Himalayan thrust belt (DeCelles *et al*., 2004) as well as detrital zircon ages from Carboniferous metasandstone units in the Qiangtang terrane (Fig. 11; Kapp *et al*., 2003a). The overall similarity in detrital zircon age distributions supports Palaeozoic plate tectonic reconstructions of northern Gondwanaland that depict a vast shallow marine sea throughout the contiguous Lhasa and Qiangtang terranes and greater India (Dewey *et al*., 1988; Leeder *et al*., 1988; Sengör & Nata'lin, 1996; Scotese, 2002).

Northern and southern provenance signatures

Data from this study and the literature suggest that it should be possible to delineate northern vs. southern detrital zircon provenance signatures in particular stratigraphic units within the Tibetan plateau. Igneous rocks in the Kunlun terrane of northern Tibet are dominated by zircon U–Pb crystallization ages ranging between ~200 and ~500 Ma, with a few ages of roughly ~930 and ~1870 Ma (Fig. 12; Gehrels *et al*., 2003a; Cowgill *et al*., 2003; Schwab *et al*., 2004). In addition to igneous rocks, sedimentary and meta-sedimentary rocks in northern Tibet have detrital zircons with age populations of ~480, ~900, ~1400 and ~1800 Ma (Fig. 13; Gehrels *et al*., 2003b). In the Songpan–Ganzi and northern Qiangtang terranes of central Tibet, zircon crystallization ages of igneous rocks are generally <220 Ma (Fig. 12). In the southern fringe of the Qiangtang terrane, igneous zircons have ages generally between ~100 and ~150 Ma (Fig. 12). In the northern part of the Himalayan thrust belt, sedimentary and meta-sedimentary rocks are dominated by detrital zircons with age populations of 500–600 and 1000–1400 Ma (Fig. 13; DeCelles *et al*., 2004; Schwab *et al*.,

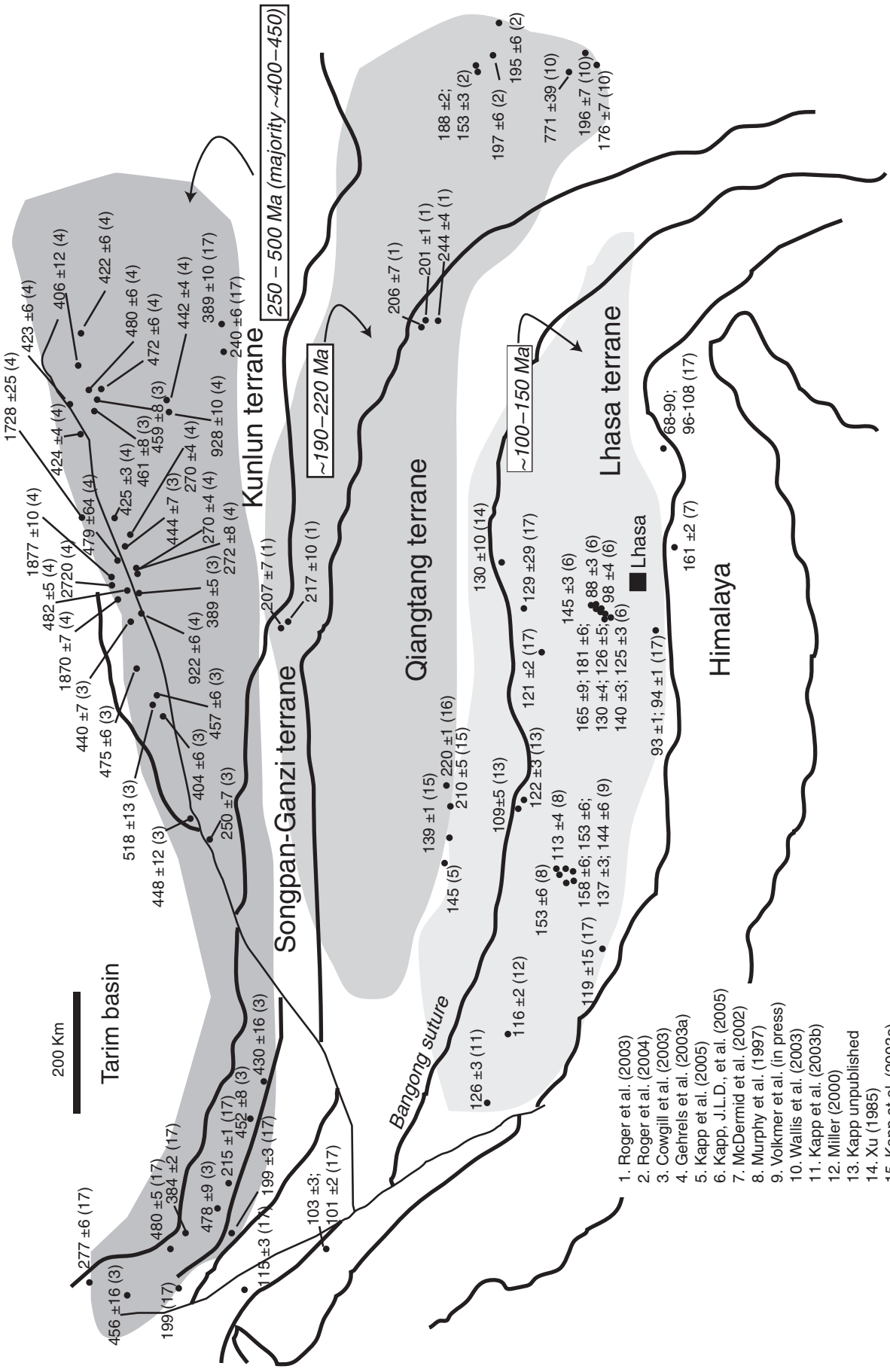

Fig. 12. Zircon uranium–lead ages of igneous rocks in the Tibetan plateau. Ages are given in Ma and the corresponding reference is denoted by the number in parentheses. Because of the large scale, the sampling sites as shown on this map (black dots) are meant to represent the approximate sampling location. The shaded regions are added to highlight general trends in the ages. The zircon crystallization ages of igneous rocks in northern Tibet are primarily between 200 and 500 Ma, and those in southern Tibet are generally < 200 Ma. The geographic distributions indicates that it may be possible to determine the first-order provenance of sedimentary rocks using detrital zircon geochronology.

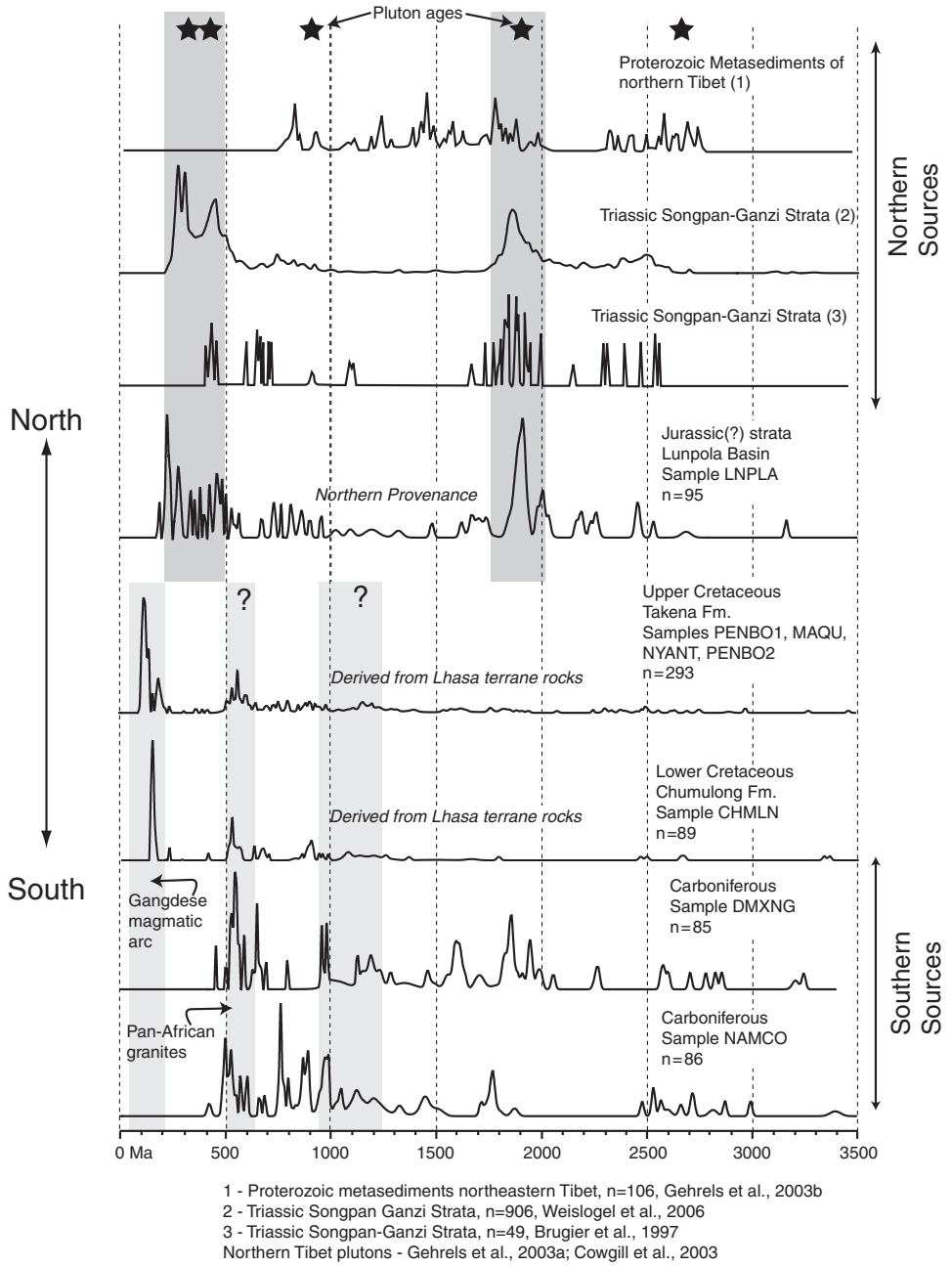

Fig. 13. Comparison of detrital zircon ages from tectonic terranes in the Himalayan–Tibetan orogenic system; the relative probability plots are ordered bottom to top as they are geographically located south to north. Prominent populations that appear to be characteristic of either the northern or southern portion of the region are highlighted. The highlighted regions with question marks represent age populations that may be present in both the north and the south. Also shown are the zircon uranium–lead ages of plutonic bodies/regions in the Tibetan plateau. The northern portion of the Tibetan plateau contains plutonic rocks that record specific periods of emplacement and cooling. The sedimentary and meta-sedimentary rocks from the northern portion of the plateau tend to have large zircon populations with ages between ~200–500 Ma and ~1700–2000 Ma. Detrital zircons with these ages are generally absent in Mesozoic sedimentary rocks in the Lhasa terrane, with the exception of the strata associated with the LNPLA sample, which was derived from northern sources (see text). Detrital zircon populations in the south have clusters in the range ~50–200, 500–600 and 1000–1400 Ma.

2004; this study). However, it must be emphasized that sources of zircons in the Himalayan thrust belt, which was part of Greater India, could not have contributed to Cretaceous rocks of the Lhasa terrane because they would have lain on the opposite of the Neotethys ocean during Cretaceous time.

The spatial differences in zircon ages on the Tibetan plateau can be exploited to assess northern vs. southern provenance signatures in Cretaceous strata of the Lhasa terrane (Fig. 13). Samples PENBO1, PENBO2, NYANT, MAQU and CHMLNG are from strata with palaeocurrent directions and petrographic characteristics that indi-

cate derivation from local sources in southern Tibet (Leier *et al*., in press). These samples contain zircon populations with ages in the range of 110–160, 500–600 and 1000–1400 Ma, which is consistent with a southern Tibetan zircon provenance signature (Figs 6 and 13). In contrast, sample LNPLA from the boundary between the Lhasa and Qiangtang terranes contains very few detrital zircons with ages of 500–600 or 1000–1400 Ma. Instead, the majority of the zircons in LNPLA have ages in the range of 200–500 and 1700–2000 Ma, which is more consistent with a northern Tibetan provenance (Fig. 13). Little additional information is available on the provenance of the strata associated with the LNPLA sample; however, palaeogeographic reconstructions of the area (Leeder *et al*., 1988; Yin *et al*., 1988) and a limited amount of palaeocurrent data from Jurassic strata near the LNPLA sampling site ($n = 28$; A. L. Leier, unpublished data) indicate southward sediment transport. In any case, the apparent differences in the detrital zircon age signatures of northern vs. southern Tibet indicate that it may be possible to use detrital zircon age distributions for distinguishing the first-order provenance of clastic stratigraphic units within the Tibetan plateau. It should be noted that many more samples are required before this hypothesis can be fully assessed and other tectonic terranes in the area (e.g. Indochina block) may play an important role in the detrital zircon signatures.

CONCLUSIONS

The scarcity of geologic data from the Tibetan plateau presents a major limitation to understanding the Cenozoic and pre-Cenozoic evolution of this region. The 743 new U–Pb detrital zircon ages presented here help to elucidate several important aspects of the geology of the Tibetan plateau and its tectono-sedimentary history, and can also be used as a point of comparison for future studies.

Many of the samples collected from the Lhasa terrane share particular populations of detrital zircon ages. Cretaceous sandstone samples contain numerous zircons with ages between 110 and 160 Ma. The Cretaceous(?) sample collected near Nam Co is the exception and lacks any zircons with ages < 400 Ma. Zircons with ages between 200 and 500 Ma are scarce in sandstone units in the Lhasa terrane, except Jurassic sandstone exposed near the Bangong suture. Detrital zircons with 500–600 Ma ages represent a substantial proportion of the total population in many of the samples. Many of the samples also contain a significant population of zircons with ages of 1000–1400 Ma. The Jurassic LNPLA sample contains a conspicuously large cluster of detrital zircons with ages of $\sim$1900 Ma, which differs from the detrital zircon age distribution in all the other samples. Almost all the samples contain a small number of zircons with ages $\sim$2500 Ma.

Several inferences and trends can be drawn from the detrital zircon data. The ages of detrital zircons from 'Lower Cretaceous' strata exposed near lake Nam Co are all older than 400 Ma, suggesting that the strata exposed along the northeastern shore of the lake are Palaeozoic in age, not Lower Cretaceous. The small number of Jurassic-age detrital zircons in Jurassic strata exposed near the Bangong suture is difficult to reconcile with the hypothesized existence of a Jurassic arc along on the southern margin of the Qiangtang terrane; however, these strata may predate the construction of the arc. These same Jurassic strata contain populations of detrital zircons with ages of 200–500 and 1800–2000 Ma, populations that are noticeably different from the ages of detrital zircons in sedimentary rocks in the southern portion of the Lhasa terrane. Differences between the age-probability plot of Jurassic strata and the geographic distribution of igneous rocks within the Tibetan plateau suggest that it might be possible to discern, at least to a first order, whether sediments were derived primarily from northern or southern Tibet. Detrital zircons in Upper Cretaceous fluvial sandstone units exposed around the city of Lhasa suggest that the southern portion of the Lhasa terrane was occupied by several distinct fluvial systems during the Late Cretaceous. The absence of any detrital zircons with ages < 100 Ma in Upper Cretaceous sandstone samples suggests that deposition of the preserved succession ceased nearer to 100 than 70 Ma. At least some of the sediment in the Upper Cretaceous strata was recycled from Palaeozoic (Carboniferous) strata that were exposed during the late Mesozoic. Similarities between Palaeozoic strata exposed in the Himalaya, Lhasa terrane and Qiangtang terrane suggest that these areas were adjacent to one another during the early–middle Palaeozoic and together composed a large portion of the northern margin of Gondwanaland.

ACKNOWLEDGEMENTS

This work was supported by the US National Science Foundation grant (EAR-0309 844), student grants from The Geological Society of America and The American Association of Petroleum Geologists and a Boren Fellowship from the US Department of Defense. Support was also provided by grants from the ExxonMobil and Chevron Corporations. This work benefited from discussions with many students and faculty members in the Department of Geosciences at the University of Arizona. We thank Ding Lin, Shundong He, Dan Eisenberg, John Volkmer, Alex Pullen, Jessica Kapp, Jen Fox, Jerome Guynn, Matt Fabijanic and our Tibetan drivers and assistants for help in the field, and Richard L. Hay for help with the petrographic work. We thank Dr Matthias Bernet and Dr Kai-Jun Zhang for their thorough and very helpful reviews.

REFERENCES

Allégre, C.J., Courtillot, V., Tapponnier, P., Hirn, A., Mattauer, M., Coulon, C., Jaeger, J.J., Achache, J., Scharer, U., Marcoux, J., Burg, J.P., Girardeau, J., Armijo, R., Gariepy, C., Gopel, C., Li, T.D., Xiao, X.C., Chang,

C.F., Li, G.Q., Lin, B.Y., Teng, J.W., Wang, N.W., Chen, G.M., Han, T.L., Wang, X.B., Den, W.M., Sheng, H.B., Cao, Y.G., Zhou, J., Qiu, H.R., Bao, P.S., Wang, S.C., Wang, B.X., Zhou, Y.X. & onghua, X. (1984) Structure and evolution of the Himalaya-Tibet Orogenic Belt. *Nature*, **307**, 17–22.

Arnaud, N., Tapponnier, P., Roger, F., Brunel, M., Scharer, U., Wen, C. & Xu, Z.Q. (2003) Evidence for Mesozoic shear along the western Kunlun and Altyn-Tagh fault, northern Tibet (China). *J. Geophys. Res.*, **108**, doi:10.1029/2001JB0904.

Burg, J-P., Proust, F., Tapponnier, P. & Ming, C.G. (1983) Deformation phases and tectonic evolution of the Lhasa block (southern Tibet, China). *Eclogae Geol. Helvet.*, **76**, 643–665.

Coulon, C., Maluski, H., Bollinger, C. & Wang, S. (1986) Mesozoic and Cenozoic volcanic rocks from central and southern Tibet: ^{39}Ar–^{40}Ar dating, petrological characteristics and geodynamical significance. *Earth Planet. Sci. Lett.*, **79**, 281–302.

Cowgill, E., Yin, A., Harrison, T.M. & Wang, X.F. (2003) Reconstruction of the Altyn Tagh fault based on U–Pb geochronology: role of back thrusts, mantle sutures, and heterogeneous crustal strength in forming the Tibetan Plateau. *J. Geophys. Res.*, **108**, doi:10.1029/2002JB02080.

Dewey, J.F., Shackleton, R.M., Chengfa, C. & Yiyin, S. (1988) The tectonic evolution of the Tibetan plateau. *Philos. Trans. Roy. Soc.Lon. Ser. A*, **327**, 379–413.

DeCelles, P.G., Gehrels, G.E., Najman, Y., Martin, A., Carter, A. & Garzanti, E. (2004) Detrital geochronology and geochemistry of Cretaceous–Early Miocene strata of Nepal: implications for timing and diachroneity of initial Himalayan orogenesis. *Earth Planet. Sci. Lett.*, **227**, 313–330.

Dickinson, W.R. & Suczek, C.A. (1979) Plate tectonics and sandstone compositions. *Am. Assoc. Petrol. Geol. Bull.*, **63**, 2164–2182.

England, P.C. & Houseman, G.A. (1986) Finite strain calculations of continental deformation 2: application to the India–Asia plate collision. *J. Geophys. Res.*, **91**, 3664–3676.

England, P.C. & Searle, M. (1986) The Cretaceous–Tertiary deformation of the Lhasa block and its implications for crustal thickening in Tibet. *Tectonics*, **5**, 1–14.

Gehrels, G.E. (2000) Introduction to detrital zircons studies of Paleozoic and Triassic strata in western Nevada and northern California. In: *Paleozoic and Triassic Paleogeography and Tectonics of Western Nevada and Northern California* (Ed. by M.J. Soreghan & G.E. Gehrels), *Geol. Soc. Am. Spec. Pap.*, **347**, 1–17.

Gehrels, G.E., Yin, A. & Wang, X.F. (2003a) Magmatic history of the northeastern Tibetan Plateau. *J. Geophys. Res.*, **108**, doi:10.1029/2002JB01876.

Gehrels, G.E., Yin, A. & Wang, X.F. (2003b) Detrital-zircon geochronology of the northeastern Tibetan plateau. *Geol. Soc. Am. Bull.*, **115**, 881–896.

Guynn, J.H., Kapp, P., Pullen, A., Heizler, M., Gerhels, G.E. & Lin, D. (2006) Tibetan basement rocks near Amdo reveal "missing" Mesozoic tectonism along the Bangong suture, central Tibet. *Geology*, **34**, 505–508.

He, S. (2005) Cretaceous–Tertiary upper crust deformation in southern Tibet. MS Thesis, University of Arizona, Tucson, 53pp.

Hu, D.G., Wu, Z.H., Jiang, W., Shi, Y.R., Ye, P.S. & Liu, Q.S. (2005) SHRIMP zircon U–Pb age and Nd isotopic study on the Nyainqentanglha Group in Tibet. *Sci. China, Ser. D-Earth Sci.*, **48**, 1377–1386.

Ingersoll, R.V., Bullard, T.F., Ford, R.L., Grimm, J.P., Pickle, J.D. & Sares, S.W. (1984) The effect of grain size on detrital modes: a test of the Gazzi-Dickinson point-counting method. *J. Sediment. Petrol.*, **54**, 103–116.

Kapp, J.L.D., Harrison, T.M., Kapp, P., Grove, M., Lovera, O.M. & Ding, L. (2005) Nyainqentanglha Shan: a window into the tectonic, thermal, and geochemical evolution of the Lhasa block, southern Tibet. *J. Geophys. Res.*, **110**, B08413, doi:10.1029/2004JB03330.

Kapp, P., Murphy, M.A., Yin, A., Harrison, T.M., Ding, L. & Guo, J. (2003a) Mesozoic and Cenozoic tectonic evolution of the Shiquanhe area of western Tibet. *Tectonics*, **22**, doi:10.1029/2001TC01332.

Kapp, P., Yin, A., Manning, C.E., Harrison, T.M. & Taylor, M.H. (2003b) Tectonic evolution of the early Mesozoic blueschist-bearing Qiangtang metamorphic belt, central Tibet. *Tectonics*, **22**, doi:10.1029/2002TC01383.

Kapp, P., Yin, A., Harrison, M.T. & Ding, L. (2005) Cretaceous–Tertiary shortening, basin development and, and volcanism in central Tibet. *Geol. Soc. Am. Bull.*, **117**, 865–878.

Kapp, P., Yin, A., Manning, C.E., Murphy, M.A., Harrison, T.M., Spurlin, M., Ding, L., Deng, X.G. & Wu, C.M. (2000) Blueschist-bearing metamorphic core complexes in the Qiangtang block reveal deep crustal structure of northern Tibet. *Geology*, **28**, 19–22.

Kidd, W.S.F., Yusheng, P., Chengfa, C., Coward, M.P., Dewey, J.F., Gansser, A., Molnar, P., Shackleton, R.M. & Yiyin, S. (1988) Geological mapping of the 1985 Chinese-British Tibetan (Xizang-Qinghai) plateau Geotraverse route. *Philos. Trans. Roy. Soc. Lond. Ser. A*, **327**, 287–305.

Leeder, M.R., Smith, A.B. & Jixiang, Y. (1988) Sedimentology, palaeoecology and palaeoenvironmental evolution of the 1985 Lhasa to Golmud Geotraverse. *Philos. Trans. Roy. Soc. Lond. Ser. A*, **327**, 107–143.

Leier, A.L., DeCelles, P.G., Kapp, P. & Gehrels, G.E. in press, Lower Cretaceous strata in the Lhasa terrane, Tibet, with implications for understanding the early tectonic history of the Tibetan plateau. *J. Sediment. Res.*

Leier, A.L., Kapp, P., DeCelles, P.G. & Ling, D. 2007 The Takena Formation of the Lhasa terrane, southern Tibet: the record of a Late Cretaceous retro-arc foreland basin. *Geol. Soc. Am. Bull.*, **119**, 31–48.

Liu, Z.Q.C. (1988) *Geologic Map of the Qinghai-Xizang Plateau and Its Neighboring Regions, Scale: 1:1 500 000*. Chengdu Institute of Geology and Mineral Resources, Geologic Publishing House, Beijing.

Ludwig, K.R. (2001) Isoplot/Ex, rev. 2.49: Berkeley Geochronology Center Special Publication 1A, 56pp.

McDermid, I.R.C., Aitchison, J.C., Davis, A.M., Harrison, T.M. & Grove, M. (2002) The Zedong terrane: a Late Jurassic intra-oceanic magmatic arc within the Yarlung-Tsangpo suture zone, southeastern Tibet. *Chem. Geol.*, **187**, 267–277.

Miller, C., Schuster, R., Kotzli, U., Frank, W. & Grasemann, B. (2000) Late Cretaceous–Tertiary magmatic and tectonic events in the Transhimalayan batholith (Kailas area, SW Tibet). *Schweiz Mineraol. Petrol.*, **80**, 1–20.

Murphy, M.A., Yin, A., Harrison, T.M., Dürr, S.B., Chen, Z., Ryerson, F.J., Kidd, W.S.F., Wang, X. & Zhou, X. (1997) Did the Indo-Asian collision alone create the Tibetan Plateau? *Geology*, **25**, 719–722.

Palmer, A.R. & Geissman, J. (1999) Geologic Time Scale, The Geological Society of America, http://www.geosociety.org/science/timescale/timescl.pdf

Pan, Y. (1993) Unroofing history and structural evolution of the southern Lhasa terrane, Tibetan Plateau: Implications for the continental collision between India and Asia, PhD Thesis, State University of New York, Albany, 287pp.

Ratschbacher, L., Frisch, W., Chen, C. & Pan, G. (1993) Deformation and motion along the southern margin of the Lhasa block (Tibet) prior to and during the India-Asia collision. *J. Geodyn.*, **16**, 21–54.

Roger, F., Arnaud, N., Gilder, S., Tapponnier, P., Jolivet, M., Brunel, M., Malavielle, J., Xu, Z. & Yang, J. (2003) Geochronological and geochemical constraints on Mesozoic suturing in east central Tibet. *Tectonics*, **22**, doi:10.1029/2002TC01466.

Roger, F., Malavielle, J., Leloup, Ph.H., Calassou, S. & Xu, Z. (2004) Timing of granite emplacement and cooling in the Songpan-Garze fold belt (eastern Tibetan Plateau) with tectonic implications. *J. Asian Earth Sci.*, **22**, 465–481.

Schwab, M., Ratschbacher, L., Siebel, W., McWilliams, M., Minaev, V., Lutkov, V., Chen, F., Stanek, K., Nelson, B., Frisch, W. & Wooden, J.L. (2004) Assembly of the Pamirs: age and origin of magmatic belts from southern Tien Shan to the southern Pamirs and their relation to Tibet. *Tectonics*, **23**, doi: 10.1029/2003TC01583.

Scotese, C.R. (2002) Earth history reconstructions: http//www.scotese.com/earth.htm

Sengör, A.M.C. & Nata'lin, B.C. (1996) Paleotectonics of Asia: fragments of a synthesis. In: *The Tectonic Evolution of Asia* (Ed. by A. Yin & T.M. Harrison), pp. 486–640. Cambridge University Press, Cambridge, UK.

Stacey, J.S. & Kramers, J.D. (1975) Approximation of terrestrial lead isotope evolution by a two-stage model. *Earth Planet. Sci. Lett.*, **26**, 207–221.

Stampfli, G.M. & Borel, G. (2004) The TRANSMED transects in space and time: constraints on the paleotectonic evolution of the Mediterranean domain. In: *The TRANSMED Atlas: The Mediterranean Region from Crust to Mantle* (Ed. by W. Cavazza, F. Roure, W. Spakman, G.M. Stampfli & P. Ziegler), pp. 53–80. Springer-Verlag Publishing, New York, NY.

Volkmer, J.E., Kapp, P., Guynn, J.H. & Lai, Q. (in press) Cretaceous–Tertiary evolution of the north-central Lhasa terrane, Tibet. *Tectonics*.

Wallis, S.R., Tsujimori, T., Aoya, M., Kawakami, T., Tereda, K., Suzuki, K. & Hyodo, H. (2003) Cenozoic and Mesozoic metamorphism in the Longmenshan orogen: implications for geodynamic models of eastern Tibet. *Geology*, **31**, 745–748.

Xu, R.H., Schaerer, U. & Allegre, C.J. (1985) Magmatism and metamorphism in the Lhasa block (Tibet): a geochronological study. *J. Geol.*, **93**, 41–57.

Yin, A. & Harrison, T.M. (2000) Geologic evolution of the Himalayan-Tibetan orogen. *Ann. Rev. Earth Planet. Sci.*, **28**, 211–280.

Yin, J., Xu, J.T., Liu, C.J. & Li, H. (1988) The Tibetan plateau: regional stratigraphic context and previous work. *Philos. Trans. Roy. Soc. Lond. Ser. A*, **327**, 5–52.

Zhang, K.J. (2000) Cretaceous paleogeography of Tibet and adjacent areas (China): tectonic implications. *Cretaceous Res.*, **21**, 23–33.

Zhang, K.J., Xia, B.D., Wang, G.M., Li, Y.T. & Ye, H.F. (2004) Early Cretaceous stratigraphy, depositional environments, sandstone provenance, and tectonic setting of central Tibet, western China. *Geol. Soc. Am. Bull.*, **116**, 1202–1222.

Manuscript received 28 August 2006; Manuscript accepted 11 June 2007.

Supplementary Material

The following supplementary material is available for this article:

Table S1. Detrital zircon raw data.

This material is available as part of the online article from: http://www.blackwell-synergy.com/doi/abs/10.1111/j.1365-2117.2007.00330.x (This link will take you to the article abstract).

Please note: Blackwell Publishing are not responsible for the content or functionality of any supplementary materials supplied by the authors. Any queries (other than missing material) should be directed to the corresponding author for the article.

